International Journal Of
Industrial Electronics Control and Optimization
Print ISSN: 3517-2645
Online ISSN: 3568-2645
Homepage: https://ieco.usb.ac.ir/

A Novel Control to Improve Dynamic Stability of Power Systems Including DFIG and SSSC

Saeed Abazari[1]| Zabihollah Faramarzi[2]
Faculty of Engineering, Shahrekord University, Shahrekord, Iran[1,2]
Corresponding author's email: saeedabazari@yahoo.com

Article Info

Article type:
Research Article

Article history:
Received: 11 Aug 2022
Received in revised form: 01 Nov 2022
Accepted: 15 Nov 2022
Published online: 30 Nov 2022

Keywords
DSC,
DFIG,
Dynamic Stability,
SSSC.

ABSTRACT

This study is concerned with the design of multi-input Dynamic Surface Control (DSC) to dynamic stability improvement of power systems which include both Doubly Feed Induction Generator (DFIG) and Static Synchronous Series Compensator (SSSC). The presented control method has a multi-input feature which acts on synchronous generators. To improve dynamic stability, the control law is developed by applying a suitable Lyapunov function. The coefficients of the proposed controller are determined by use of metaheuristic optimization algorithms. This optimal control law leads to a significantly improved performance in comparison with linear control. A particular low-pass filter is also introduced and applied to cancel the effects of additional undesired terms in the design method, leading to a simplified control form compared to the other available approaches in the literature. Implementing an adaptive parameter estimation scheme will result in the robustness of the proposed method. The effectiveness of the presented approach is investigated on a standard 39-Bus power system which includes DFIG and SSSC.

I. Introduction

In today's world, there is a tremendous attention to implement new sources of energy. Of particular importance, the renewable energy resources such as wind energy are at the main center of research and practical efforts. Due to the fact that the wind velocity varies with time, the DFIGs are introduced to extract maximum electrical power from wind-turbines [1, 2].

Considering load demands growth, it is quite desirable to transmit higher level of electrical power through the existing electrical transmission networks. On the other hand, dealing with the issues such as dynamic stability, insulations components, and thermal capacity of the current electrical networks all together limits the maximum possible level of electric power transmission. Moreover, the safety, technical difficulties and high cost of constructing new electrical transmission lines, reduce the possibility of expanding new transmission lines. Hence, implementing Flexible AC Transmission Systems (FACTS) to increase the capacity of the existing power networks has been rapidly attracted researcher's attentions. Among FACTS devices, SSSC is one of the sophisticated and favorable in increasing the capacity of the transmission line [3-5]. In the SSSC structure, passive elements are not employed. High level of switching mode in SSSC results in injection and absorption of active electrical power with low cost and high speed [6].

Dynamic stability of power system is one of important aspects of power system operation, which usually occurs after unwanted disturbances. In power systems equipped with SSSC and DFIG elements, dynamic stability could be further improved [7, 8]. Traditionally, Power System Stabilizers (PSS) have been used to stimulate synchronous generators. The application of PSSs to improve dynamic stability is widely studied and investigated in the recent decades. However, due to their weak local performance and occurring of problems such as Sub-Synchronous Resonance (SSR), applying PSSs is very limited. Most of the PSS design methods are based on the assumption of considering a local linear model of the power

Copyright © 2022 Abazari et al. Published by University of Sistan and Baluchestan. This work is licensed under a Creative Commons Attribution-Noncommercial 4.0 International license. (https://creativecommons.org/licenses/by-nc/4.0/). Non-commercial uses of the work are permitted, provided the original work is properly cited
DOI: 10.22111/IECO.2022.41721.1416

network and small signal analysis. In some recent papers, Linear Matrix Inequalities (LMIs) technique is applied to suitably place the eigenvalues of the assumed local linear models in certain points in order to improve the dynamic stability. However, due to the high intrinsic nonlinearity nature of the power networks, the mentioned approach does not guarantee the robustness of dynamic stability against parameter variations, [9, 10].

Beside the complexity in the nonlinear methods design, compared to the previous approaches applying nonlinear methods leads to robust and high-quality results. These nonlinear methods reduce sensitivity of the overall system to variations in the parameters [11, 12]. In [13], nonlinear back-stepping approach to stimulate the synchronous generators was developed to improve dynamic stability. However, DFIG and SSSC components was not implemented. A fuzzy DSC scheme was applied in the design method of [14]. However, the proposed method is limited to vary the synchronous generators stimulation field circuit. In [15-16], DFIG and SSSC components was separately employed to stimulate synchronous generators. In the current study, to improve the dynamic stability, utilizing both DFIG and SSSC devices together with nonlinear adaptive multi-input DSC method is proposed. The effects of control signals on each other and on the performance of the power system are also considered. Moreover, the parameters of the designed control law are optimized by use of intelligent algorithms in order to improve the stability. A low-pass filter is introduced in the design scheme to cancel the undesired terms in control law and to prevent large variations in control signals. Also, implementing the adaptive law for unknown parameters leads to the robustness against parameters variations.

In this paper, firstly the assumed models for DFIG and SSSC are introduced. Then, based on a third-order model for synchronous generators, a generic model for the overall power network is offered. Finally, an adaptive multi-input DSC control law is developed. The results of implementing the proposed approach are verified by performing time domain simulations implemented on the 10-machine New England test system which also includes DFIG and SSSC. The results are compared with two linear and nonlinear approaches in the literature.

TABLE 1
SI BASE UNITS

SYMBOL	VARIABLE NAME
δ_i	Rotor angle of ith generator
ω_i	Rotor speed of ith generator
$\acute{E}_{qi}$	Internal voltage of ith generator in q-axes
$\acute{E}_i$	Internal voltage of ith generator
I_{di}	Stator current of ith generator in d-axis
I_{qi}	Stator current of ith generator in q-axis
u_{fi}	Excitation voltage of ith generator
M_i	Moment of inertia of ith generator
P_{mi}	Mechanical input power of ith generator
u_d	Signal control of DFIG
TABLE 1 CONTINUED	
δ_{0i}	Rotor angle of ith generator in steady state
ω_{0i}	Rotor speed of i ith generator in steady state
V_i	Amplitude of Generator terminal voltage ith
Θ_i	Phase of Generator terminal voltage ith
$\acute{T}_{d0i}$	Constant time generator excitation coil ith
x_{di}	d-axis reactance generator steady state ith
$\acute{x}_{di}$	d-axis reactance generator transient state ith
x_{qi}	q-axis reactance generator steady state ith
X_i	EQUIVALENT REACTANCE OF DFIG IN STEADY STATE
$\acute{X}_i$	EQUIVALENT REACTANCE OF DFIG IN TRANSIENT STATE

II. Power System Modeling

A. DFIG Modelling

Figure 1. depicts the multi-machine power system including DFIG. The DFIG consists of Rotor Side Converter (RSC) and Grid Side Converter (GSC). Since the RSC plays the main role in stability improvements, the presented model is based on controlling this converter inputs. In the literature, this model is known as the synchronous generator model for DFIG. In this model, it is assumed that the stator resistance is zero. Hence, the following equations will represent the DFIG dynamic, see [17]:

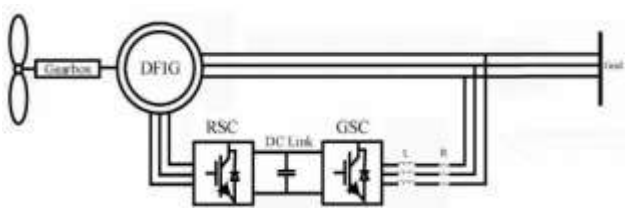


Fig 1. DFIG Connected to a Multi-Machine Network [1]

$$\begin{cases} \dot{\delta}_i = \frac{1}{\acute{E}_{qi}T_{0i}}(-T_{0i}(\omega_i-\omega_0)\acute{E}_{qi} - \frac{X_i-\acute{X}_i}{\acute{E}_{qi}T_{0i}}V_i sin(\delta_i-\theta_i) \\ \qquad +T_{0i}\omega_0(u_{d1i}cos(\delta_i)+u_{d2i}sin(\delta_i))] \\ \dot{\omega}_i = \frac{\omega_0}{2H_i}[P_{mi}\frac{\omega_s}{\omega_i} - B_{ij}\acute{E}_{qi}V_i\sin(\delta_i-\theta_i)] \\ \dot{\acute{E}}_i = \frac{1}{T_{0i}}(-\frac{X_i}{\acute{X}_i}\acute{E}_{qi} + \frac{X_i-\acute{X}_i}{\acute{X}_i}V_i cos(\delta_i-\theta_i) \\ \quad +T_{0i}\omega_0(u_{d1i}sin(\delta_i)+u_{d2i}cos(\delta_i))]) \end{cases} \quad (1)$$

where, V_i و θ_i are the amplitude and phase angle of the connected bus voltage, respectively. B_{ij} is the susceptance of admittance matrix between the DFIG and the connected buses. $\acute{E}_i$ represents the internal voltage of ith generator. V_{ri} و Φ_{ri} are respectively, the amplitude and the phase angle of the applied voltage to the DFIG rotor in polar coordinates. Finally, u_{d1i} and u_{d2i} are DFIG control inputs, which lead to the improvements in dynamic stability [17,18].

B. SSSC Model

The series converter is the applied model for SSSC. This converter injects active-power to the series link which leads to the dynamic stability improvement of connected buses

voltages. According to the Fig.2, it is assumed that SSSC is placed between the ith and jth buses [19,20].

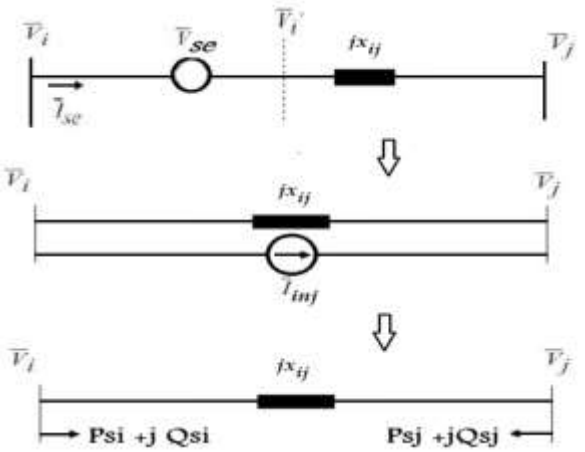


Fig. 2. a. SSSC between bus I and bus j b. equivalent circuit of SSSC c. Alternative equivalent injection model of SSSC in power system

It is possible to model the SSSC performance with a series voltage source. This series voltage, V_{se}, is controlled by the following equations:

$$\begin{cases} \bar{I}_{inj} = -jB_{ij}V_{se} \\ v_{se} = V_{se}e^{j\Phi_{se}} \\ B_{ij} = \frac{1}{x_{sij}} \end{cases} \quad (2)$$

In the presented analysis method, the SSSC is replaced by its equivalent injection model in the considered power system. The resulted configuration is depicted in Fig. 2.c. In this figure, the injected power are P_{si}، P_{sj} ، $Q_{si}$and Q_{sj} for ith and jth buses [21]:

$$\begin{cases} P_{si} = -B_{ij}V_{se}V_i \,\text{SIN}(\Theta_i - \Phi_{se}) \\ Q_{si} = B_{ij}V_{se}V_i \,\text{COS}(\Theta_i - \Phi_{se}) \\ P_{sj} = B_{ij}V_{se}V_j \,\text{SIN}(\Theta_j - \Phi_{se}) \\ Q_{sj} = -B_{ij}V_{se}V_j \,\text{COS}(\Theta_j - \Phi_{se}) \end{cases} \quad (3)$$

In this study, it is assumed that SSSC is only able to generate and consume reactive power. Therefore, its total active power generation and consumption must be zero. Since the series resistance of the of transmission lines, in which the SSSC is took places, is negligible, the SSSC voltage can be represented by the following equations:

$$\Phi_{se} = tan^{-1}\left(\frac{V_j \,\text{SIN}(\Theta_j) - V_i \,\text{SIN}(\Theta_i)}{V_j \,\text{COS}(\Theta_j) - V_i \,\text{COS}(\Theta_i)}\right) \quad (4)$$

C. *TOTAL POWER SYSTEM MODEL INCLUDING SYNCHRONOUS GENERATORS, DFIG, AND SSSC*

Fig.3 shows the general schematic of a power system network which includes Synchronous Generators, DFIG, and SSSC. This network consists of n1 synchronous generators, one DFIG and one SSSC. It is assumed that the mechanical input power of synchronous generators is constant. The stator's resistances are also assumed to be negligible. The total power in ith bus is modeled by $Y_i = G_i - jB_i$.

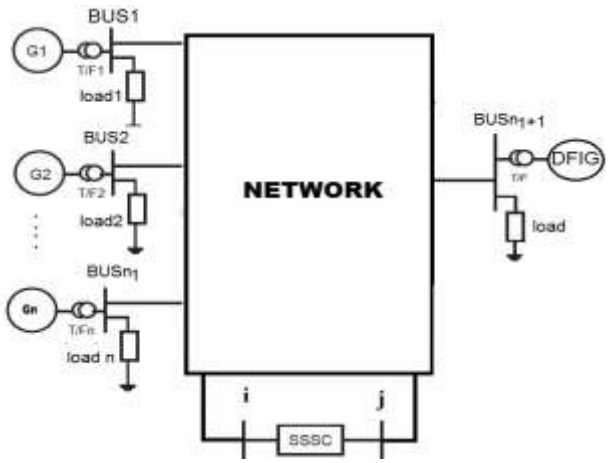


Fig.3. The Assumed Overall Power System Network

The considered model for each synchronous generator is a third-degree-equation which is described in (5). In (5), u_{fi} is the control input of the generators, see [22]:

$$\begin{cases} \dot{\delta}_i = \omega_i - \omega_0 \\ \dot{\omega}_i = \frac{1}{M_i}[P_{mi} - \acute{E}_{qi}I_{qi}] \\ \dot{\acute{E}}_{qi} = \frac{1}{\acute{T}_{doi}}\left(u_{fi} - \acute{E}_{qi} - (x_{di} - \acute{x}_{di})I_{di}\right) \end{cases} \quad (5)$$

The combination of the algebraic power balance equations of all connected buses to the synchronous generators with DFIG equations, in addition to the injected power of SSSC models will result in the following equations of the whole power system network model:

$$\begin{cases} \dot{\delta}_i = \omega_i - \omega_{0i} \\ \dot{\omega}_i = \frac{1}{M_i}[P_{mi} - \acute{E}_{qi}I_{qi}] \\ \dot{\acute{E}}_{qi} = \frac{1}{\acute{T}_{doi}}(u_{fdi} - \acute{E}_{qi} - (x_{di} - \acute{x}_{di})I_{di}) \end{cases} \quad (6)$$

$$\begin{cases} \dot{\delta}_i = \frac{1}{\acute{E}_i T_{0i}}\left[-T_{0i}(\omega_i - \omega_0)\acute{E}_i - \frac{X_i - \acute{X}_\iota}{\acute{E}_{qi}T_{0i}}V_i \sin(\delta_i - \theta_i)\right) \\ \qquad +T_{0i}\omega_0(u_{d1i}cos(\delta_i) + u_{d2i}sin(\delta_i))] \\ \dot{\omega}_i = \frac{\omega_0}{2H_i}[P_{mi}\frac{\omega_s}{\omega_i} - B_i\acute{E}_i V_i \sin(\delta_i - \theta_i) \\ \dot{\acute{E}}_i = \frac{1}{T_{0i}}[-\frac{X_i}{\acute{X}_\iota}\acute{E}_i + \frac{X_i - \acute{X}_\iota}{\acute{X}_\iota}V_i cos(\delta_i - \theta_i) \\ \qquad +T_{0i}\omega_0(u_{d1i}sin(\delta_i) + u_{d2i}cos(\delta_i))] \end{cases} \quad (7)$$

$$\begin{cases} \dot{V}_i = \sum_{j=1}^{N} c_{ij}H_j + \sum_{j=1}^{N} d_{ij}u_{fj} + \sum_{j=1}^{N} k_{ij}\,r \\ \dot{\Phi}_i = \sum_{j=1}^{N} c_{i+n+2,j}H_j \\ \quad + \sum_{j=1}^{N} d_{i+n+2,j}u_{fj} + \sum_{j=1}^{N} k_{i+n+2,j}\,r \end{cases} \quad (8)$$

In above, (6) is the assumed dynamic model for synchronous generators, (7) is for the DFIG part and (8) describes the buses voltages of SSSC. N is the number of all the connected buses to the synchronous generators, DFIG and the connected buses to the SSSC. $B_{ij}{}'s$ are the elements of the reduced order admittance matrix of the power system network, where:

$$\begin{cases} \dot{\delta} = [\dot{\delta}_1 \,..\, \dot{\delta}_{n1} \quad \dot{\delta}_d]^T \\ \dot{U}_s = \begin{bmatrix} \dot{u}_{s1} \\ \dot{u}_{s2} \end{bmatrix} = \begin{bmatrix} r_1 \\ r_2 \end{bmatrix} = r \\ \dot{E}_q = \left[\dot{E}_{q1} \,..\, \dot{E}_{qn1} \quad \dot{E}\right]^T \\ \dot{v} = [\dot{V}_1 \,..\, \dot{V}_{n+2} \quad \dot{\theta}_1 .. \quad \dot{\theta}_{n+2}]^T \\ h_i = \frac{1}{T_{oi}}(-\acute{E}_{qi} - (X - \acute{X})I_{di}) \\ H = [h_1 .. \quad h_{n1}]^T \end{cases} \quad (9)$$

It should be noticed that r_1 and r_2 are related to each other, therefore, only one control input will be considered for SSSC. U_f is:

$$U_f = [\ u_{f1} \quad \cdots u_{fn1} \quad u_{d1}\ ]^T \quad (10)$$

$$\begin{cases} \dot{X}_1 = X_2 \\ \dot{X}_2 = M_{inv}[P_m - X_3] \\ \dot{X}_3 = F_T + U + \Gamma\varphi \end{cases} \quad (11)$$

WHERE:

$$U = G_T U_f + Lr \quad (12)$$

$$\begin{cases} X_1 = [x_{11}\ x_{12}\ ..\ x_{1n}]^T \\ X_2 = [x_{21}\ x_{22}\ ..\ x_{2n}]^T \\ X_3 = [x_{31}\ x_{32}\ ..\ x_{3n}]^T \\ X_{3s} = [x_{3d1}\ x_{3d2}\ ..\ x_{3dn}]^T \\ \varphi = [x_{d1} - \acute{x}_{d1}\ x_{d2} - \acute{x}_{d2} \quad ....\ x_{dn} - \acute{x}_{dn}]^T \\ \Gamma = \begin{bmatrix} \Gamma_1(X_1, X_2, X_3) & \cdots & 0 \\ \vdots & \ddots & \vdots \\ 0 & \cdots & \Gamma_n(X_1, X_2, X_3) \end{bmatrix} \end{cases} \quad (13)$$

WHERE IN (13), $x_{1i} = \delta_i - \delta_i{}^*$, $x_{2i} = \omega_i - \omega_i{}^*$ AND

$$x_{3i} = \begin{cases} \frac{\acute{E}_{qi}V_i sin(\delta_i - \Theta_i)}{\acute{x}_{di}} + \frac{{V_i}^2 sin2(\delta_i - \Theta_i)}{2x_{qi}\acute{x}_{di}}(\acute{x}_{di} - x_{qi}) & 1 \le i \le n1 \\ \frac{\acute{E}_i V_i \mathrm{SIN}(\delta_i - \theta_i)}{\acute{x}_{di}} & n1 + 1 \le i \le n \end{cases}$$

AND

$$\Gamma_i = \begin{cases} \frac{-(\acute{E}_{qi} - V_i \mathrm{COS}(\delta_i - \theta_i))}{\acute{x}_{di}T_{0i}} & 1 \le i \le n1 \\ \frac{V_i}{\acute{X}_i T_{0i}}(\mathrm{COS}(\delta_i - \theta_i) + \frac{\mathrm{SIN}(\delta_i - \theta_i)\,\mathrm{COS}(\delta_i)}{\mathrm{SIN}(\delta_i)}) & n1 + 1 \le i \le n \end{cases}$$

Here, n is the total number of the generators including synchronous and DFIG ones. Since it is assumed that only one DFIG is in the considered power system, n1, the number of synchronous generators, equals n-1.

III. Design of Nonlinear Adaptive Multi-Input DSC Control Law

In this section, based on the described model for power system network developed in Section 2, together with DSC method and adding an adaptive scheme for estimating uncertain parameters, a multi-input control law will be designed. In this framework, the following equations are formulated [23]:

$$\begin{cases} Z_1 = X_1 \\ Z_2 = X_2 - X_{2d} \\ Z_3 = X_3 - X_{3d} \end{cases} \quad (14)$$

Based on the DSC method, the function x_{2d} is determined in such a way that x_1 stabilizes and x_{3d} stabilizes x_2.

where:

$$Z_1 = [z_{11}\ z_{12}\ ..\ z_{1n}]^T, Z_2 = [z_{21}\ z_{22}\ ..\ z_{2n}]^T \quad (15)$$

We then have:

$$\begin{cases} \dot{Z}_1 = X_2 \\ \dot{Z}_2 = M_{inv}[P_m - X_3] - \dot{X}_{d2} \\ \dot{Z}_3 = F_T + U + \Gamma\varphi - \dot{X}_{d3} \end{cases} \quad (16)$$

$$\begin{cases} \tau_2\dot{X}_{2d} + X_{2d} = \bar{X}_2 \\ \tau_3\dot{X}_{3d} + X_{3d} = \bar{X}_3 \end{cases} \quad (17)$$

Now, in the following steps, a suitable Lyapunov function is defined which leads to the design of final control law [24, 25]:

Step #1:

$$V_{z1} = \frac{1}{2}{Z_1}^T Z_1 \quad (18)$$

$$\dot{V}_{z1} = {Z_1}^T(Z_2 + X_{2d} - \bar{X}_2 + \bar{X}_2) \rightarrow \bar{X}_2 = -K_D Z_1 \quad (19)$$

$$\dot{V}_{z1} = -{Z_1}^T K_D Z_1 - {Z_1}^T(\bar{X}_2 - X_{2d}) + {Z_1}^T Z_2$$

Step #2:

$$V_{z2} = V_{z1} + \frac{1}{2}{Z_2}^T Z_2 \quad (20)$$

$$\begin{aligned} \dot{V}_{z2} &= -{Z_1}^T K_D Z_1 - {Z_1}^T(\bar{X}_2 - X_{2d}) + {Z_1}^T Z_2 \\ &+ {Z_2}^T(M_{inv}[P_m - X_3] - \dot{X}_{2\mathrm{d}}) \\ &= -{Z_1}^T K_D Z_1 - {Z_1}^T(\bar{X}_2 - X_{2d}) + {Z_2}^T(Z_1 \\ &+ M_{inv}[P_m - Z_3 - X_{3d} + \bar{X}_3 - \bar{X}_3] - \dot{X}_{2\mathrm{d}}) \\ &= -{Z_1}^T K_D Z_1 - {Z_1}^T(\bar{X}_2 - X_{2d}) + {Z_2}^T(Z_1 \\ &\quad + M_{inv}[P_m - \bar{X}_3] - \dot{X}_{2\mathrm{d}}) \\ &- {Z_2}^T M_{inv} Z_3 - {Z_2}^T M_{inv}(\bar{X}_3 - X_{3d}) \end{aligned} \quad (21)$$

It is assumed that:

$$Z_1 + M_{inv}[P_m - \bar{X}_3] - \dot{X}_{2\mathrm{d}} = -K_T Z_2 \quad (22)$$

which in equations (19) and (22) K_D and K_T are arbitrary positive definite matrices.

$$\rightarrow \bar{X}_3 = {M_{inv}}^{-1}(K_T Z_2 + M_{inv} P_m + Z_1 - \dot{X}_{2\mathrm{d}}) \quad (23)$$

Considering Equation (19) we have:

$$\dot{V}_{z2} = -{Z_1}^T K_D Z_1 - {Z_1}^T(\bar{X}_2 - X_{2d}) - {Z_2}^T K_T Z_2 - {Z_2}^T M_{inv}(\bar{X}_3 - X_{3d}) - {Z_2}^T M_{inv} Z_3$$

Step #3:

$$V_{z3} = V_{z2} + \frac{1}{2}{Z_3}^T Z_3 + \frac{1}{2}\tilde{\varphi}^T \gamma \tilde{\varphi} \quad (24)$$

$$\dot{V}_{z3} = \dot{V}_{z2} + {Z_3}^T \dot{Z}_3 + \gamma^{-1}\tilde{\varphi}^T \tilde{\varphi}$$

$$\dot{V}_{z3} = \dot{V}_{z2} + {Z_3}^T(F_T + U + \Gamma\varphi - \dot{X}_{3\mathrm{d}}) + \tilde{\varphi}^T \gamma \dot{\tilde{\varphi}}\ )$$

$$\dot{V}_{z3} = -{Z_1}^T K_D Z_1 - {Z_1}^T(\bar{X}_2 - X_{2d}) - {Z_2}^T K_T Z_2 - {Z_2}^T M_{inv}(\bar{X}_3 - X_{3d}) - {Z_2}^T M_{inv} Z_3 + {Z_3}^T(F_T + U + \Gamma\varphi - \dot{X}_{3\mathrm{d}}) + \tilde{\varphi}^T \gamma \dot{\tilde{\varphi}}\ )$$

$$\dot{V}_{z3} = -{Z_1}^T K_D Z_1 - {Z_1}^T(\bar{X}_2 - X_{2d}) - {Z_2}^T K_T Z_2 - {Z_2}^T M_{inv}(\bar{X}_3 - X_{3d}) + {Z_3}^T(F_T + U + \Gamma\varphi - \dot{X}_{3\mathrm{d}} - M_{inv} Z_2) + \dot{\tilde{\varphi}}^T \gamma \tilde{\varphi}$$

$$\dot{V}_{z3} = -{Z_1}^T K_D Z_1 - {Z_1}^T(\bar{X}_2 - X_{2d}) - {Z_2}^T K_T Z_2 - {Z_2}^T M_{inv}(\bar{X}_3 - X_{3d}) + {Z_3}^T(F_T + U + \Gamma\varphi - \dot{X}_{3\mathrm{d}} - M_{inv} Z_2) + \dot{\tilde{\varphi}}^T \gamma \tilde{\varphi} \quad (25)$$

It should be noted that $\tilde{\varphi} = \varphi - \hat{\varphi}$:

$$\dot{V}_{z3} = -{Z_1}^T K_D Z_1 - {Z_1}^T(\bar{X}_2 - X_{2d}) - {Z_2}^T K_T Z_2 - {Z_2}^T M_{inv}(\bar{X}_3 - X_{3d}) + {Z_3}^T(F_T + U + \Gamma\hat{\varphi} - \dot{X}_{3\mathrm{d}} - M_{inv} Z_2) + ({Z_3}^T \Gamma + \dot{\tilde{\varphi}}^T \gamma) \quad (26)$$

Since, φ is constant, then $\dot{\varphi} = 0$, hence, $\dot{\tilde{\varphi}} = -\dot{\hat{\varphi}}$. In order to make a negative value for the derivative of Lyapunov function, the following relations should be applied:

$$\begin{cases} (F_T + U + \Gamma\hat{\varphi} - \dot{X}_{3\mathrm{d}} - M_{inv} Z_2) = -K_s Z_3 & (27-a) \\ ({Z_3}^T \Gamma - \dot{\hat{\varphi}}^T \gamma) = 0 & (27-b) \end{cases}$$

Where K_s is positive definite matrix, The following relation is obtained:

$$U = -K_s Z_3 - F_T - \Gamma\hat{\varphi} + \dot{X}_{3d} + M_{inv} Z_2 \quad (28)$$

$$({Z_3}^T \Gamma - \dot{\hat{\varphi}}^T \gamma) = 0 \rightarrow \dot{\hat{\varphi}} = {\gamma^{-1}}^T \Gamma Z_3 \quad (29)$$

If the backstepping method is applied, the control input will be obtained from (26).

$$U = -K_s Z_3 - F_T - \Gamma\hat{\varphi} + M_{inv} Z_2 + {M_{inv}}^{-1}(K_T(M_{inv}[P_m - X_3] - \dot{X}_{2\mathrm{d}}) + M_{inv}\dot{P}_m + Z_2 + X_{2d} - \dot{X}_{2\mathrm{d}} \quad (30)$$

It should be mentioned that the number of terms in (28) is fewer than those ones in (30).

According to (28) for the control input, the derivative of Lyapunov function will be:

$$\dot{V}_{z3} = -{Z_1}^T K_D Z_1 - {Z_2}^T K_T Z_2 - {Z_3}^T K_s Z_3 - {Z_1}^T(\bar{X}_2 - X_{2d}) - {Z_2}^T M_{inv}(\bar{X}_3 - X_{3d}) \quad (31)$$

The complete proof is described in Appendix A.There are a number of controller coefficients in (28). In order to design these coefficients, a PSO algorithm will be applied. PSO algorithm in comparison with most of the other intelligent methods is formulated in simple manner. It is a memory-based algorithm and has a higher convergence rate [26].

The cost function considered for optimization by PSO method is selected as follows:

$$J = \sum_{j=1}^{n}(\delta_i - \delta_{i0})^2 + \tau \sum_{j=1}^{n}(\omega_i - \omega_{i0})^2 \quad (32)$$

In relation (32), τ is a weight coefficient that can be determined experimentally.

The designed control system block is shown in Fig. 4. In this control diagram, first the output states of the main plant are sampled and then entered into the parameter estimator and adaptive backstepping controller with the DSC filter. In this block, the appropriate estimation of the uncertain parameters of the system is produced and sent back to the main controller. In the DSC adaptive backstepping controller block, the DSC filter provides the derivative value of the desired values in the design of the backstepping controller without the calculation needed for direct derivation and sends it back to the backstep controller. Finally, the appropriate input control signals to improve the dynamic stability of the power generation system are generated and fed into the DFIG and SSSC.

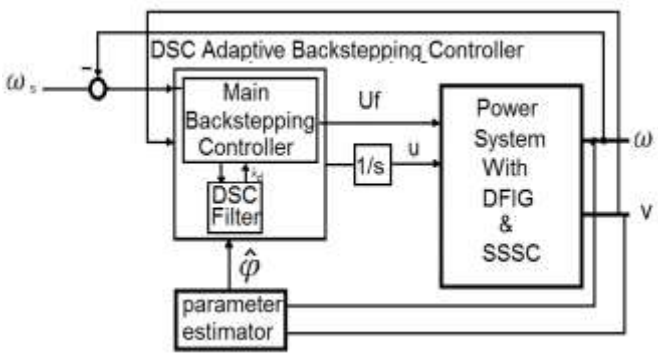


Fig 4. Control diagram and Power System Including DFIG and SSSC Applying Multi-Input Adaptive DSC

A. *The proposed Algorithm for Dynamic Stability Improvement of Power System Including DFIG and SSSC*

Fig. 5 describes the proposed control algorithm for the stability improvements of the power system which includes synchronous generators, DFIG and SSSC.

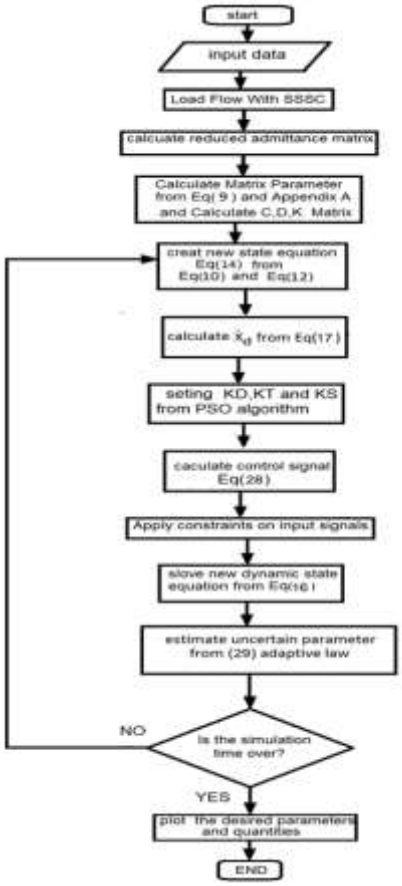


Fig 5. Flowchart Simulation of the Power System Including DFIG and SSSC with Applying Multi-Input Adaptive DSC

IV. Simulation Results

In order to investigate the effectiveness of the proposed control law, a stability analysis in different scenarios is considered for the 10-machine New England test system. This power system is depicted in Fig.6. It includes 10 synchronous machines, one DFIG in Bus 19, and one SSSC component between Bus 6 and Bus 7. The initial data for this system is developed in [27].

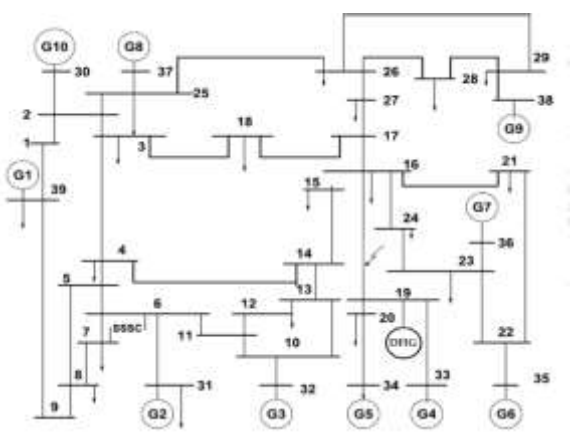


Fig 6. The NEW ENGLAND standard 39-bus power system includes a wind generator equipped with DFIG

In this case-study, a 3-phase short-circuit fault in the vicinity of generator 4 is occurred and lasted for 100 milliseconds. Fig.7 shows the variations in the speed of the G4 and DFIG under the condition in which no control input is employed. It is clear that the power system is dynamically unstable. Now, by applying the proposed control law, the deviations of internal angle and speed of G4 and DFIG are depicted in Fig. 8 and Fig.9. As it can be seen from these figures, the angle and the speed of the rotor reach to their stable condition in about 2 seconds after clearing the fault. Fig.10 shows the behavior of internal angles and angular velocities of the generators of this power system. For a better investigation of the power system damping, the phase diagram for G4 and the DFIG is depicted in Fig.11. It can be seen that the system tends toward its stable condition very fast. Fig.12 show the control input signal for all the machines, DFIG, and SSSC. This figure shows that the amplitudes of all the signals are limited and they reach to their initial values. In Fig.13, the estimation of the unknown parameters of the power system is depicted. It shows that the estimation error tends to zero, and estimation values reach to their references.

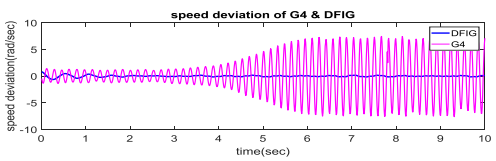
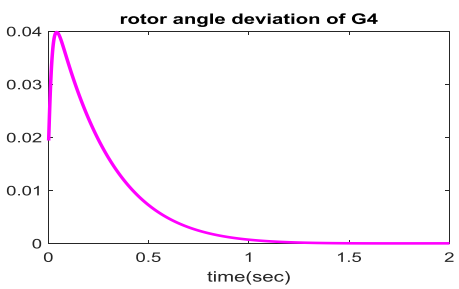
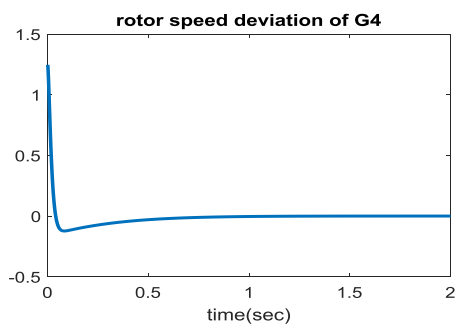


Fig 7. Speed deviation G4 and DFIG while is not control on system

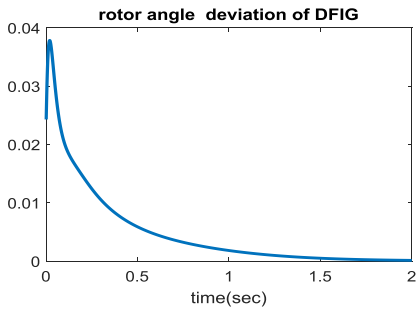


(a)

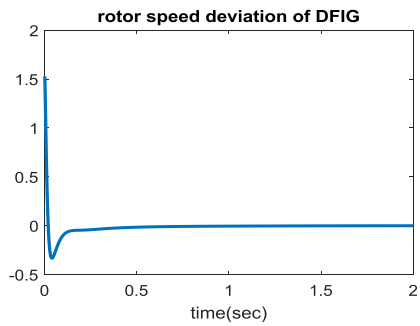


(b)

Fig 8. (a)rotor angle deviation for G4, (b)Speed deviation for G4 after fixing the short circuit error

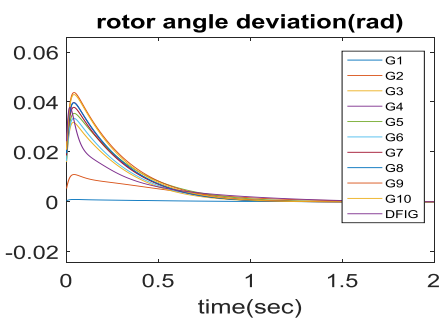


(a)

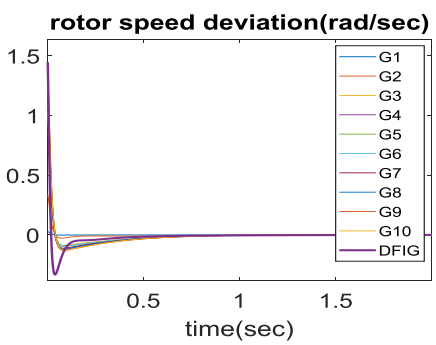


(b)

Fig 9. (a)rotor angle deviation for DFIG, (b)Speed deviation for DFIG after fixing the short circuit



(a)



(b)

Fig 10. rotor angle deviation of the generators rotor after fixing the short circuit error in bus39 Rotor Speed deviation of all generators after the short circuit fault in bus 39

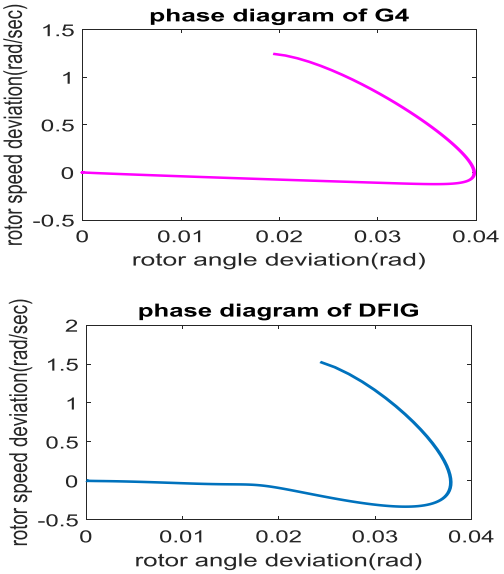


Fig.11. phase diagram of wind turbine based DFIG and G4

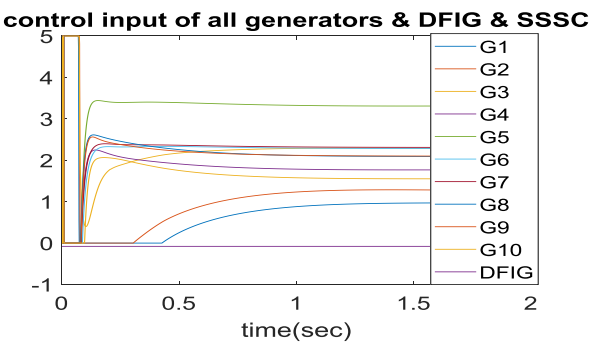


Fig 12. control signals of G4 and DFIG, SSSC by Multi input dynamic surface control

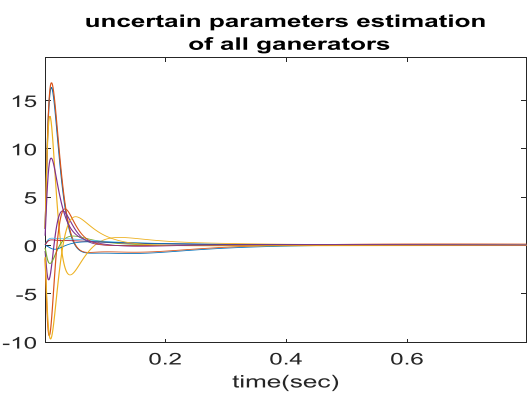


Fig 13. estimation of uncertain parameter for all generators and DFIG

It should be mentioned that the input mechanical power to the generators may vary with time. This condition more frequently happens in Wind-Turbines. Therefore, in order to make a more comprehensive scenario, it is assumed that the mechanical input power to the DFIG suddenly change about 10% and then reach to its initial value. In Fig.14 the variation

in angle and speed of DFIG rotor is depicted. It shows that the controller acts in a correct manner and make the signal amplitude to reach to its stable condition in a short period of time.

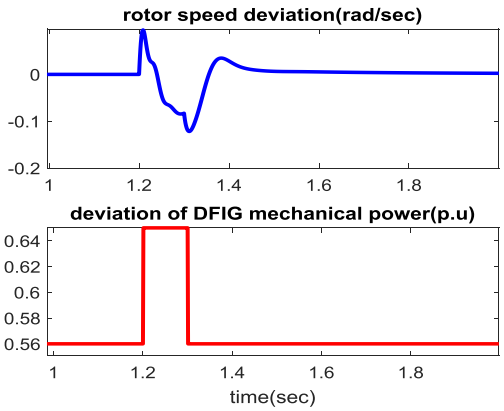


Fig 14. speed deviation of synchronous generator and DFIG against changing point of fault occurrence to near G7

In the Fig.15 to compare the performance of the controller adesigned by the DSC method, the results obtained with the backtracking method are compared. It can be seen that the DSC controller has a better performance for the speed and internal angle diagrams of the generator In addition, this filter softens the response and In Fig.16, for the input signal of G4, a comparison is made between the applied backstepping control approach and the proposed control scheme. It is observed that by use of the proposed control law, the trajectories reach to its stable condition in a faster way with lower overshoot value with respect to controller signal obtained from applying backstepping method. In addition, this filter softens the response as shown in the figure and makes us without the need for derivation.

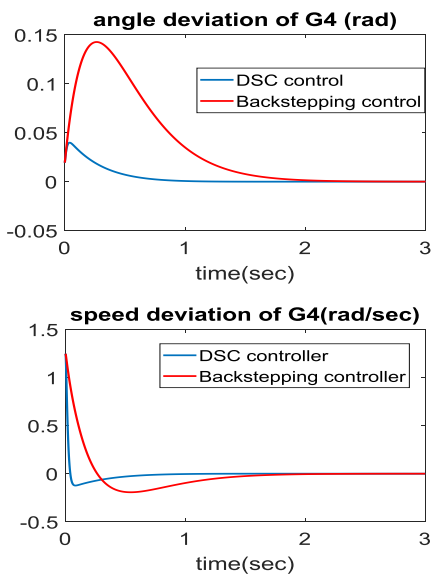


Fig.15.comparing rotor angle and speed deviation G4 in back stepping and DSC methods after the short circuit fault in bus 39

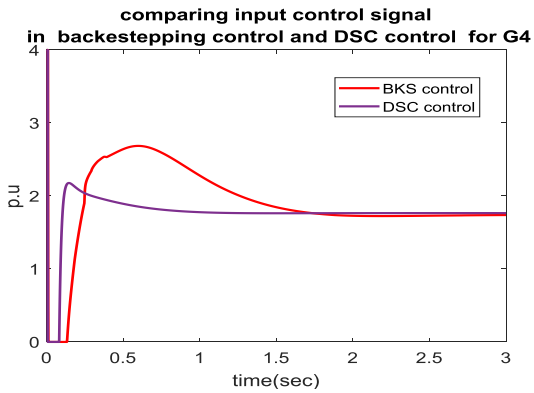


Fig 16. comparing control input signal for G4 in back stepping and DSC methods

In order to further examine the performance of the proposed control law with the other important controller design methods, a comparison is made in Table 2. It is obtained from the information in this table that the proposed method has a superior performance with respect to the linear scheme of [13]. In Table 3, the proposed control law is compared with the nonlinear method offered in [9]. The results show that the proposed control law has a better performance with respect to the results obtained from [9].

TABLE 2
COMPARISON OF CONTROL CRITERIA BETWEEN ADAPTIVE MULTI-INPUT DYNAMIC SURFACE CONTROL AND OPTIMIZED LINEAR CONTROL METHOD IN [13]

	Proposed control in this article			Optimized Linear Control Design in [13]		
G4	Rise time (Sec.)	settling time (Sec.)	Over shoot (p.u.)	Rise time (Sec.)	settling time (Sec.)	Over shoot (p.u.)
Speed dev	0.08	0.7	0.1	0.2	4.5	0.15
Rotor ang	1.50	2.0	2.29˚	0.15	4.0	25˚
Ctrl signal	0.15	1.1	2.1	-	-	-

TABLE 3
COMPARISON OF CONTROL CRITERIA BETWEEN ADAPTIVE MULTI- INPUT DYNAMIC SURFACE CONTROL WITH BACKSTEPPING CONTROL METHOD IN [9]

	Proposed control in this article			Nonlinear Control design in [9]		
G3	Rise time (Sec.)	settling time (Sec.)	Over shoot (p.u.)	Rise time (Sec.)	settling time (Sec.)	O shoot (p.u.)
Speed dev	0.05	0.9	0.12	0.5	5.0	0.5
Rotor angle	1.10	1.8	1.5˚	0.1	5.0	13˚
Ctrl signal	0.08	1.0	1.8	0.4	7.5	3.2

V. Conclusions

In this study, a multi-input adaptive DSC control law is developed to improve dynamic stability of the power system including DFIG and SSSC. The simulation results show the superiority of the proposed control law in improvement the dynamic stability with respect to backstepping method (Table 3) and linear methods (Table 2). For instance, according to Table 3, the overshoot is improved by 50% and the settling time is improved by 20% with respect to the recent reported results of applying backstepping scheme. The performance of the designed control law with respect to the unknown parameter variation and also rapid change in mechanical input of DFIG shows the robustness properties of the proposed control law. In other word, the control signal also has a smooth form with respect to the corresponding signals from backstepping controllers developed in the recent literature.

REFERENCES

[1] S. Muller, M.Deicke & R I K W, "doubly-fed induction generator systems for wind turbines", IEEE Industry Applications Magazine, June 2002.

[2] H.S.Koa,G.G. Yoonb, N.H. Kyunga,W.Pyo Hongc, "Modeling and control of DFIG-based variable-speed wind-turbine",Electric Power Systems Research 78, pp:1841–1849, 2008.

[3] N. G. Hingorani and L. Gyugyi, "Understanding FACTS, Concepts and Technology of Flexible AC Transmission Systems," IEEE Press, 2000.

[4] B. K. Dubey, N.K. Singh," Multi machine power system stability enhancement with UPFC using linear quadratic regulator techniques", International Journal of Advanced Research in Engineering and Technology, Vol.11, Issue 4, pp. 219-229, April 2020.

[5] Y. Chi, Y. Xu," Multi-objective robust tuning of STATCOM controller parameters for stability enhancemnt of stochastic wind-penetrated power systems", IET Generation, Transmission & Distribution, Sep 2020.

[6] A. Movahedia, A.Halvaei Niasara, G. Gharehpetianb, " Designing SSSC, TCSC, and STATCOM controllers using AVURPSO, GSA, and GA for transient stability improvement of a multi-machine power and GA for transient stability improvement of a multi-machine power system with PV and wind farms system with PV and wind farms, " Elsevier, Electrical Power and Energy Systems, Vol. 106 , pp. 455–466, 2019.

[7] M. A. Mahmud, "An alternative LQR-based excitation controller design for power systems to enhance small-signal stability," International Journal of Electrical Power & Energy Systems ,Vol. 63, pp. 1–7, Dec 2014.

[8] W. Du, X. Chen, H, Wang, "Parameter tuning of the PLL to consider the effect on power system small-signal angular stability," IET Renewable. Power Generation., Vol. 12, No. 1, pp. 1-8, 2018.

[9] T. K. Roy, M. A. Mahmud, Amanullah M. T. Oo," Robust Adaptive Back stepping Excitation Controller Design for Higher-Order Models of Synchronous Generators in Multi machine Power Systems", Transactions on Power Systems, IEEE, 2018.

[10] Y. Liu, Q. H. Wu, H. Kang, X. Zhou, "Switching Power System Stabilizer and Its Coordination for Enhancement of Multi-machine Power System Stability," CSEE journal of power and energy systems, Vol. 2, No. 2, June 2016.

[11] M. A. Mahmud, M. J. Hossain, H. R. Pota, and A. M. T. Oo," Robust Partial Feedback Linearizing Excitation Controller Design for Multimachine Power Systems", 0885-8950 (c) 2015 IEEE.

[12] T. Parida, S. Dhar,N. Nayak, "A finite time adaptive back-stepping sliding mode control for instantaneous active-reactive power dynamics based DFIG-wind generation towards improved grid stability ", Wind Energy published by John Wiley & Sons Ltd, 2020 .

[13] M.Maleki, S.Abazari," Dynamic Stability Improvement of Power System With Simulation and Coordinated Control of DFIG and UPFC using LMI", International Journal of Industrial Electronics,Control and optimization,vol.4,NO.3,pp.341-353,July.2021.

[14] G. Zhu, L. Nie, M.Zhou ,X.Zhang, L.I. Sun,CH.Zhang, "Adaptive Fuzzy Dynamic Surface Control for Multi-Machine Power System Based on Composite Learning Method and", IEEE Access, September 18, 2020.

[15] A. Saleem Mir and N. Senroy, "DFIG damping controller design using robust CKF based adaptive dynamic programming",IEEE Transactions on Sustainable Energy, 2018.

[16] F.A.L.Jowder,''Influence of mode of operation of the SSSC on the small disturbance and transient stability of a radial power system,'' IEEE Transactions on Power Systems, vol.20, Issue. 2, May 2005.

[17] K. Elkington, V.Knazkins, M. Ghandhari, "On the stability of power systems containing doubly fed induction generator-based generation, " Elsevier, Electric Power Systems Research, vol. 78,No. 9 , pp. 1477–1484, September 2008.

[18] S.Ghaedi, S.Abazari, and G.Arab-Markadeh, "Novel nonlinear control of DFIG and UPFC for transient stability increment of power system". IET Generation, Transmission & Distribution, Vol.16, No.19, pp.3799-3813, 2022.

[19] P. R. Sahu, P. K. Hota, S. Panda, " Power system stability

enhancement by fractional order multi input SSSC based controller employing whale optimization algorithm ," Science Direct**,** Journal of Electrical Systems and Information Technology , Vol. 5, No 3, pp. 326-336 , December 2018.

[20] M. Noroozian, M.Ghandehari, "Improving Power System Dynamics By Series-Connected FACTS Device,". IEEE Transactions on Power Delivery, Vol. 12, No. 4, October 1997.

[21] Z.Faramarzi, S.Abazari, S.Hoghoughi and N.R.Abjadi "Dynamic stability improvement of power system with DFIG using multi-input backstepping control" Electrical Engineering, pp.1-17, 2022.

[22] P. Kundur, "Power System Stability and Control," New York, NY, USA: McGraw-Hill, 1994.

[23] G. Zhu, L. Nie, M.Zhou ,X.Zhang, L.I. Sun,CH.Zhang ,'' Adaptive Dynamic Surface Control for Servo System Driven by Twin Motors With Unknown Actuator Failures,'' IEEE Access August 23, 2019.

[24] H. K.Khalil, "Nonlinear systems", Upper Saddle River, NJ: Prentice Hall, 2002.

[25] E.Slotine, W.Li, "Applied Nonlinear Control ", Published by Prentice Hall, 1991.

[26] J.Ma, D.Zhao, Y.Shen and A.G.Phadke," Research on Positioning Method of Low Frequency Oscillating Source in DFIG-Integrated System with Virtual Inertia Control", IEEE Transactions on Sustainable Energy, IEEE, 2019.

[27] O. Moradi, S. Abazari, N.Mahdi "Robust Sliding Mode-based UPQC for Transient Conditions in Weak Islanded Networks", International Journal of Industrial Electronics, Control and Optimization, Vol.4,pp.267-276,2021.

Appendix A:

Proof:

It can be shown that:

$\tau_2\dot{X}_{2d} + X_{2d} = \bar{X}_2$,

$\tau_3\dot{X}_{3d} + X_{3d} = \bar{X}_3$

Define the following variables:

$$\begin{cases} Y_1 = X_{2d}\text{-}\bar{X}_2 \\ Y_2 = X_{3d}\text{-}\bar{X}_3 \end{cases} \quad (a.1)$$

According to a.1One can obtain:

$$\dot{Y}_1 = -\frac{Y_1}{\tau_2}\text{-}\dot{\bar{X}}_2 = -\frac{Y_1}{\tau_2} + L_1$$

$$\dot{Y}_2 = -\frac{Y_2}{\tau_3}\text{-}\dot{\bar{X}}_2 = -\frac{Y_2}{\tau_3} + L_2$$

Where-$\dot{\bar{X}}_2 = L_2$*and* -$\dot{\bar{X}}_3 = L_3$. $|L_i|$ has a maximum value L_{iM} on a compact region. Therefore, $|L_i| \le L_{iM}$. Based on the Young inequality- the following inequalities can be written:

$$Y_i^T\dot{Y}_i = -\frac{Y_i^TY_i}{\tau_{i+1}} + Y_i^TL_i \le -\frac{Y_i^TY_i}{\tau_{i+1}} + |Y_i^T||L_i| \le -\frac{Y_i^TY_i}{\tau_{i+1}} + \frac{1}{2T}L_{iM}{}^2Y_i^TY_i + \frac{T}{2} \quad (a.2)$$

T is a positive definite diagonal matrix, Now a Lyapunov function is defined as (a.3):

$$V_{zn} = V_{z3} + Y_1^TY_1 + Y_2^TY_2 \quad (a.3)$$

Let consider equation (a.3), the derivative of the Lyapunov function and replace $\dot{V}_{z3}$ from(31) can be written as:

$$\dot{V}_{zn} = -Z_1^TK_DZ_1\text{-}Z_2^TK_TZ_2\text{-}Z_3^TK_sZ_3 + Z_1^TY_1 + Z_2^TM_{inv}Y_2 + Y_1^T\dot{Y}_1 + Y_2^T\dot{Y}_2 \quad (a.4)$$

Now by using (a.2) in (a.4) results in:

$$\dot{V}_{z3} \le -Z_1^TK_DZ_1\text{-}Z_2^TK_TZ_2\text{-}Z_3^TK_sZ_3 + Z_1^TY_1 + Z_2^TM_{inv}Y_2\text{-}\frac{Y_1^TY_1}{\tau_2} + \frac{1}{2T}L_{1M}{}^2Y_1^TY_1 + \frac{T}{2}\text{-}\frac{Y_2^TY_2}{\tau_3} + \frac{1}{2T}L_{2M}{}^2Y_2^TY_2 + \frac{T}{2}$$

On the other hand, based on Young inequality,

$$Z_1^TY_1 \le \frac{Z_1^TZ_1}{2} + \frac{Y_1^TY_1}{2},\ Z_2^TM_{inv}Y_2 \le \frac{Z_2^TZ_2}{2} + \frac{Y_2^TM_{inv}{}^2Y_2}{2} \quad (a.5)$$

Considering (a.5) and (a.4),

$$\dot{V}_{z3} \le -Z_1^TK_DZ_1\text{-}Z_2^TK_TZ_2\text{-}Z_3^TK_sZ_3 + \frac{Z_1^TZ_1}{2} + \frac{Y_1^TY_1}{2} + \frac{Z_2^TZ_2}{2} + \frac{Y_2^TM_{inv}{}^2Y_2}{2}\text{-}\frac{Y_1^TY_1}{T_2} + \frac{1}{2T}L_{1M}{}^2Y_1^TY_1 + \frac{T}{2}\text{-}\frac{Y_2^TY_2}{T_3} + \frac{1}{2T}L_{2M}{}^2Y_2^TY_2 + \frac{T}{2}$$

$$\dot{V}_{z3} \le -Z_1^T(K_D\text{-}\frac{I}{2})Z_1\text{-}Z_2^T(K_T\text{-}\frac{I}{2})Z_2\text{-}Z_3^T(K_s)Z_3\text{-}Y_1^T(-\frac{I}{2} + \frac{I}{T_2}\text{-}\frac{1}{2T}L_{1M}{}^2)Y_1\text{-}Y_2^T(-\frac{M_{inv}{}^2}{2} + \frac{I}{T_3}\text{-}\frac{1}{2T}L_{2M}{}^2)Y_2 + T$$

$$a = \min\left\{K_D\text{-}\frac{I}{2}, K_T\text{-}\frac{I}{2}, K_s, -\frac{I}{2} + \frac{I}{\tau_2}\text{-}\frac{1}{2T}L_{1M}{}^2, -\frac{M_{inv}{}^2}{2} + \frac{I}{\tau_3}\text{-}\frac{1}{2T}L_{2M}{}^2\right\}$$

$b = \{T\}$

$\dot{V}_{z3} \le -aV_{z3} + b$

$V_{z3}(t) \le (V_{z3}(t_0)\text{-}\frac{b}{a})e^{-a(t-t_0)} + \frac{b}{a} \le V_{z3}(t_0) + \frac{b}{a}, \forall t \ge t_0$

From this inequality one can conclude that by suitable choosing of coefficients, the Lyapunov function and therefore the magnitude of errors, could be made smaller and smaller as desired.



Saeed Abazari Received his BS degree in electrical engineering from Esfahan in 1989 , the MSc degree from Ferdowsi university ,Mashad,Iran In 1992, and the PhD degree from Sharif university,Thehran,Iran in 2002.Currently in electrical engineering Department at the university of Sharekolrd,Shahrekord of Iran.His research interests are electrical power distribution system, smart grid, and protection.



Zabihollah Faramarzi Received his BS degree in electrical engineering from Amirkabir university,Tehran,Iran in 2006 , the MSc degree from Esfahan university , Iran In 2013, and the PhD degree from Shahrekord university,Iran in 2021.His research interests are power system stability with renewable energy and FACTS, nonlinear control in power system, and nonlinear control in power electronic.